Simple and universal model for electron-impact ionization of complex biomolecules

Hong Qi Tan, Zhaohong Mi, and Andrew A. Bettiol
Centre for Ion Beam Applications, Department of Physics, National University of Singapore, Singapore 117551

(Received 22 August 2017; published 7 March 2018)

We present a simple and universal approach to calculate the total ionization cross section (TICS) for electron impact ionization in DNA bases and other biomaterials in the condensed phase. Evaluating the electron impact TICS plays a vital role in ion-beam radiobiology simulation at the cellular level, as secondary electrons are the main cause of DNA damage in particle cancer therapy. Our method is based on extending the dielectric formalism. The calculated results agree well with experimental data and show a good comparison with other theoretical calculations. This method only requires information of the chemical composition and density and an estimate of the mean binding energy to produce reasonably accurate TICS of complex biomolecules. Because of its simplicity and great predictive effectiveness, this method could be helpful in situations where the experimental TICS data are absent or scarce, such as in particle cancer therapy.

DOI: 10.1103/PhysRevE.97.032403

I. INTRODUCTION

Particle cancer therapy is gaining increasing popularity and has a significant advantage over traditional x-ray-based therapy due to the localized energy deposition of the energetic particles at the Bragg peak [1]. As such, in recent decades there have been increasing efforts in understanding and modeling the fundamental interaction between radiation and biological targets in cells and tissues [2]. The very first step of such modeling relies on calculating the cross sections of the interaction between radiation and biomolecules. In fact, one of the main modes of radiation damage in cells is the direct effect on DNA, which involves the direct interaction of secondary electrons (induced by incident energetic particles) with the DNA's backbone or nucleotide bases [3,4]. It is therefore necessary to evaluate the total ionization cross section (TICS) for the direct interaction between electrons and the biomolecules, which could provide input data for better understanding and modeling effort [5–7].

However, reliable models and methods to evaluate the TICS of electrons with various complex biomolecules such as DNA and proteins, to our knowledge, are scarce. As a matter of fact, a notable universal semiempirical method that relies only on a small amount of input information on the biomolecules has been successfully employed for proton particle impact [8,9]. The extension of the method used for proton impact to electron impact is challenging. On the one hand, exchange interaction needs to be considered as both the incident and target particles are electrons and are indistinguishable from a quantum-mechanics point of view. On the other hand, contrary to the proton case, we are interested in both high-energy and low-energy incident electrons (below 1 keV). The former is produced mainly in the proximal region and the latter near the Bragg peak [10–12] during particle cancer therapy. The low-energy incident particle implies that the energy level structures of the target biomolecules need to be considered. Thus a more detailed expression for the binding energy effects needs to be devised.

Here we present a simple and universal semiempirical method to evaluate the TICS of electrons with different biomolecules, based on extending the models used for proton impact [8,9]. We will show that the outright application of the method for proton impact to electron impact leads to severe deviation from the experimental and other theoretical results and thus further modification needs to be made. However, significantly, after taking the exchange interaction and the low-energy electrons into account, the calculation results are consistent with those results published elsewhere. In addition, to evaluate the practical utility of such a method, a parameter sensitivity assessment is carried out to understand the accuracy of the cross section when certain parameters are unknown or estimated. It is anticipated that the work presented in this paper could advance the understanding of ion-induced biological effects in particle cancer therapy.

II. THE BASIC SEMIEMPIRICAL MODEL FOR ELECTRON IMPACT IONIZATION

Based on the dielectric formalism, a universal semiempirical model has been successfully employed to calculate the TICS of various complex biological targets after proton impact [8,9]. We investigate whether this model could be extended to electron impact after considering the exchange interaction nature of electrons as well as the efficacy of impacting low-energy electrons. The calculation of the TICS begins with the expression of the single differential cross section (SDCS), which is calculated using the dielectric formalism [13]. In this formalism, the important quantity is the energy-loss function (ELF) which is given by $\mathrm{Im}[-\frac{1}{\epsilon(k,E)}]$, where ϵ is the complex dielectric function and k and E are the wave number and energy transferred during electronic excitation. The main advantage of the dielectric formalism is that if the ELF is experimentally measured for the entire range of k and E of the Bethe surface, the result will inherently contain information on the electronic excitation spectrum of the material and the collective or many-body interactions of the material with the projectile. The

expression of the SDCS for the electronic ith shell is given by [14,15].

$$\frac{d\sigma_i}{dW} = \frac{4\pi e^2}{h^2}\frac{m}{TN}\int_{k_1}^{k_2}\frac{dk}{k}\mathrm{Im}\left[-\frac{1}{\epsilon(k,B_i+W)}\right], \quad (1)$$

where T is the kinetic energy of the electron projectile, W is the energy of the ejected electron, N is the number of target atoms or molecules per unit volume, B_i is the binding energy of the ith shell electrons, and m is the mass of the electron. The minimum and maximum momentum transfer are manifest in the integration limits $k_1 = \frac{2\pi\sqrt{2m}}{h}(\sqrt{T} - \sqrt{T-E})$ and $k_2 = \frac{2\pi\sqrt{2m}}{h}(\sqrt{T} + \sqrt{T-E})$, where E is the energy transferred from the projectile to the target and $E = W + B$. The SDCS depends on the density of the material ρ through the parameter N.

The challenging part of the dielectric formalism is evaluating the ELF over the entire Bethe surface. One can use quantum chemistry methods but will be more computationally involved and time-consuming for a large database of proteins [16,17]. The most common way is to measure the ELF in the optical limit where $k \to 0$ and extend the ELF over the entire k space using the extension algorithms [18]. The optical energy loss function (OELF), $\epsilon(0,E)$, can be measured using x-ray spectroscopy [19] or other methods [20]. This method is regarded as semiempirical method in the literature as the determination of the OELF is wholly empirical, whereas the extension algorithm to the full Bethe surface is based on theoretical formulas. Finally, to determine the TICS, the ELF is split into different contributing electronic shells involving excitation and ionization. OELF has been measured extensively for elements and some commonly encountered materials in material science, but little has been done on biomaterials. However, Tan *et al.* [21,22] have developed a semiempirical way to estimate the OELF of organic biomaterial based on only the chemical composition of the materials. Their method is based on the fact that there is an intense peak between 20 to 25 eV for the 13 organic biomaterials that were measured and can be approximated by a single Drude function in the energy range 0–40 eV as

$$\mathrm{Im}\left[-\frac{1}{\epsilon(0,E)}\right] = \frac{a(Z)E}{[E^2 - E_p(Z)^2]^2 + \gamma^2E^2}. \quad (2)$$

The parameter $E_p(Z)$ represents the peak position and is dependent on the atomic number Z and γ represents the width of the Lorentz function. They can both be evaluated easily using the following parametrization [21]:

$$E_p = (19.927 + 0.9807\bar{Z})\ \mathrm{eV}, \quad (3)$$

$$\gamma = (13.741 + 0.3215\bar{Z})\ \mathrm{eV}, \quad (4)$$

where $\bar{Z}$ is the mean atomic number of the biomolecule. The scaling parameter $a(Z)$, which is also dependent on Z, can be evaluated by imposing the f-sum rule [23] over the entire energy range. For energy more than 50 eV, the OELF can be obtained from the photoabsorption data from Ref. [24]. Finally, the gap between 40 eV and 50 eV is matched by fitting with a quadratic function. This concludes the first step of the method. This method is extended to DNA bases and other biomaterials in Refs. [8,25]. The semiempirical OELF agrees well with most biomolecules and deduces accurately the peak position of the OELF for energy less than 50 eV.

For the second step, several extension algorithms have been developed over the years. In the original model proposed, a simple quadratic dispersion relation was assumed for the E_p parameter and no dispersion relation for γ [25]. This simple extension algorithm has been shown to produce reasonably accurate SDCS and TICS for protons impacting DNA bases [8,9]. However, in this paper, we use the Mermin's extension algorithm [26,27] partly due to its success in predicting ionization cross-section of dry DNA by ions [28,29]. This extension algorithm is based on random-phase approximation (RPA). There are approaches which goes beyond RPA [30–32] by taking into account explicit electron-electron interaction but will be more computationally costly to use with a huge database of protein materials. The Mermin-type ELF (MELF), ϵ_M, is given by:

$$\mathrm{Im}\left[\frac{-1}{\epsilon(\omega,k)}\right]_{\mathrm{MELF}} = \sum_i \frac{A_i}{\omega_i^2}\mathrm{Im}\left[\frac{-1}{\epsilon_M(\omega,k;\omega_i,\gamma_i}\right], \quad (5)$$

where A_i, γ_i, and ω_i are determined from experimental fitting to OELF. ϵ_M is the Mermin dielectric function given by:

$$\epsilon_M = 1 + \frac{(1 + i\gamma\hbar/\omega[\epsilon_L(k,\omega + i\gamma) - 1]}{1 + (i\gamma\hbar/\omega)[\epsilon_L(k,\omega + i\gamma) - 1]/[\epsilon_L(k,0) - 1]}, \quad (6)$$

where ϵ_L is the Lindhard dielectric function [13], γ is the plasmon damping factor, and $\omega = E/\hbar$. In the optical limit where $k \to 0$, ϵ_M approaches the single Drude function as in Eq. (2).

Last, instead of splitting the ELF into various energy shell contribution, Ref. [8] uses a simple approximation that yields result agreeing well with experimental data. A single mean binding energy $\bar{B}$ is used to describe the outer-shell ionization of biomolecules. Thus, an outer-shell electron will be ionized if $E > \bar{B}$ and the ejected electron will have energy $W = E - \bar{B}$. The mean binding energy is calculated from the arithmetic mean of the binding energy of different energy shells. The choice of a single mean binding energy means that error will arise from improperly assigning some excitations as ionizations and vice versa. This error is negligible by the following argument: In the case of liquid water exposed to high-energy projectiles which are capable of ionizing all outer-shell electrons, the mean binding energy of water is about 18 eV and, according to Ref. [14], most of the ionization takes place above this energy and the excitation contribution is little. Thus, there will be only a small error on the estimated TICS. Furthermore, the difference between the mean binding energy and the actual ionization energy in the molecule is of the order of several eV which can be neglected during the Monte Carlo simulation with secondary electrons. The effect will be more pronounced with low-energy electrons as the mean free path varies the greatest when the secondary electron energy is uncertain [21]. To circumvent this issue, one can set the production energy cutoff at 10 eV while using this model in Monte Carlo simulation. In Sec. III, physical corrections specific to electron projectiles will be introduced before arriving at the final TICS.

III. EXTENDED MODEL FOR ELECTRON IMPACT IONIZATION

For proton projectiles, the above procedure will suffice for the evaluation of the SDCS and TICS in biomolecules. However, as we have indicated, electron projectiles need to be treated differently. This section will focus on describing the corrections needed to calculate the TICS for electron impact. Experimental data on SDCS are scarce for electron impact ionization but not TICS. In particular, experimental TICS data of DNA bases measured in condensed state was published very recently [33]. In our approach, the TICS can be calculated from the SCDS by using Eq. (8), and the theoretical calculation results are then compared with experimental data and other theoretical results,

$$\sigma = \int_B^{E'} \frac{d\sigma}{dE} dE, \tag{7}$$

$$= \frac{4\pi e^2}{h^2} \frac{m}{TN} \int_B^{E'} \int_{k_1}^{k_2} \mathrm{Im}\left[-\frac{1}{\epsilon(k,E)}\right] \frac{dk}{k} dE, \tag{8}$$

where $E' = T$, which is the maximal energy to be transferred to electron. The extension of the proton-projectile method used for ion impact to one appropriate for electron impact is not trivial because of exchange interaction and interest in low-energy electrons where binding energy of each shell needs to be factored in. To solve the first problem, we used the exchange interaction formula derived by Ritchie *et al.* [34], which is an analogy of the Mott cross section [14], as follows:

$$\frac{d\sigma_{\mathrm{ex}}}{dE}(E,T) = \frac{d\sigma}{dE}(E,T) + \frac{d\sigma}{dE}(T+B-E,T) - \left(1-\sqrt{\frac{B}{T}}\right) \times \left[\frac{d\sigma}{dE}(E,T)\frac{d\sigma}{dE}(T+B-E,T)\right]^{1/2}. \tag{9}$$

The upper integral limit of the exchange interaction cross section is $E' = (T+B)/2$ in Eq. (8). It is important to note that no exchange and correlation effect is considered between the screening electrons in the current work for simplicity, scalability, and rapid calculation. This effect has been modelled and reported in Refs. [30–32] and has shown to result in 40% larger inelastic mean free path (IMFP) than pure RPA approach for liquid water.

For the second problem, to produce accurate cross sections of low-energy incident electrons, we need to take into account the binding energy of each shell. However, any model that requires the individual binding energies of the electronic shells as input parameters will make the model too complicated for practical use. Here we introduce a correction to the mean binding energy in the form:

$$\bar{B}(T) = B_0 + \frac{k}{T}, \tag{10}$$

motivated by the fact that the Rutherford cross section is proportional to $1/T$. B_0 and k are input parameters in this mean binding energy correction formula. In the limit of large incident energy, $\bar{B}(T) \approx B_0$, which is the mean binding energy proposed in Ref. [25] and is equal to 18.13 eV for water. When the incident energy is small, $\bar{B}$ is dependent on the kinetic energy of the projectile T to take into account the sensitivity

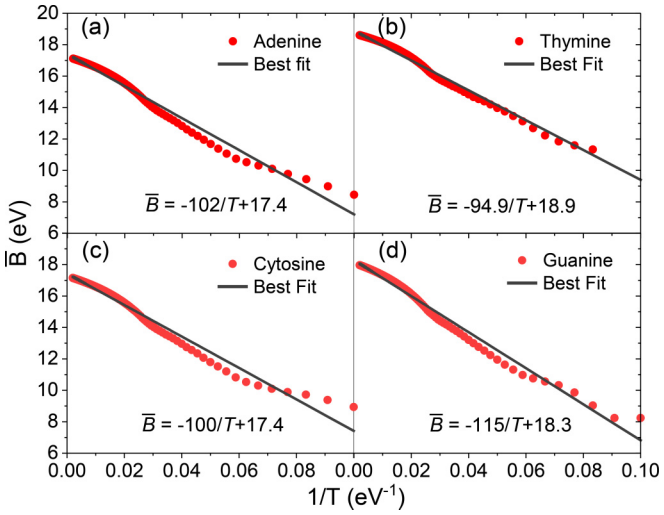

FIG. 1. Theoretical calculation and fitting of the mean binding energy of (a) adenine, (b) thymine, (c) cytosine, and (d) guanine at different energy of incident electrons. The red dots show the mean binding energy calculated by using Eqs. (11) and (12) with various incident energy of the electrons. The solid lines show the best fit lines with formula expressed in Eq. (10).

to shell structure at low energy. This arises due to the lower (or zero) cross section in ionizing shell with higher binding energy than the incident kinetic energy. To estimate the parameters B_0 and k of the DNA bases, we evaluate $\bar{B}$ according to the following:

$$\bar{B}(T) = \frac{\Sigma_i B_i \sigma_i(B_i,T)}{\Sigma_i \sigma_i(B_i,T)}, \tag{11}$$

$$\sigma_i(B_i,T) = \int_0^{T-B_i} \frac{4\pi a_0^2 R^2 N_e}{T} \frac{1}{(B_i+W)^2} dW, \tag{12}$$

and use the binding energy data from Ref. [35].

The index i labels the energy levels in the molecule. The cross section given in Eq. (12) is assumed to be of the Rutherford-scattering form [36] for simplicity but will be shown to yield sufficiently accurate results for the ionization cross section. The parameter a_0 represents the Bohr radius (0.052918 nm), R is the Rydberg energy (13.6057 eV), and N_e is the number of electrons in each subshell.

Using the binding energy data from Ref. [35] and assuming N_e to be constant, the mean binding energies expressed in Eq. (11) are evaluated at different incident energy for the four DNA bases and are shown in Fig. 1. The results are then fitted with the expression in Eq. (7) to estimate the parameters B_0 and k. It is evident from Fig. 1 that the average binding energy expression for the 4 DNA bases can be fitted well with the proposed mean binding energy correction formula expressed by Eq. (10). The fitting parameters B_0 and k are also quite similar in all four DNA bases. Thus, using this semiempirical fit for the mean binding energy, we maintain the simplicity of the method without the inclusion of the entire binding energy spectrum as input. The decrease in $\bar{B}$ with lower incident energy will increase both the ionization and excitation contribution towards TICS. However, for DNA bases, the electronic excitation cross sections reported in Ref. [37] is

about 10^{-17} cm^2 (for electron incident energy up to 18 eV), which is an order of magnitude smaller than the ionization cross section. This suggests that a decrease in $\bar{B}$ will result in an increase in the accuracy of the TICS estimation.

IV. RESULTS AND DISCUSSION

Calculations were made to find the electron-impact TICS of the four DNA bases by using both the original model and and our model with the two extensions described in Secs. II and III. The results are shown in Fig. 2. The TICS curves plotted are based on the combination of the modifications made to the original method, i.e., with considering exchange correlation and (or) energy-dependent binding energy. For comparison to validate the efficacy of the extended model, the experimental data which are the first published measurement of electron-impact TICS for the four DNA bases [33] are also plotted in Fig. 2. The curve in green is the result of applying the method from Ref. [25] and is seen to deviate the most from the experimental result. The curves in green and blue are the result of using a constant binding energy and they do not give any information on the TICS for incident electron energies less than 20 eV. The addition of the exchange interaction for the electrons decreases the TICS values in general and the experimental data agree best with the model after the addition of both the exchange interaction and new binding energy formula corrections as shown by the yellow curve. Thus, with the modifications discussed in Sec. III, we have managed to produce the TICS of electron impact on biomaterials that agrees well with the experimental data from 10 eV to 500 eV with maximal difference of up to 10% being observed in guanine.

The new semiempirical method developed in this paper for electron impact ionization is also compared with various other theoretical methods for evaluating the TICSs of DNA bases

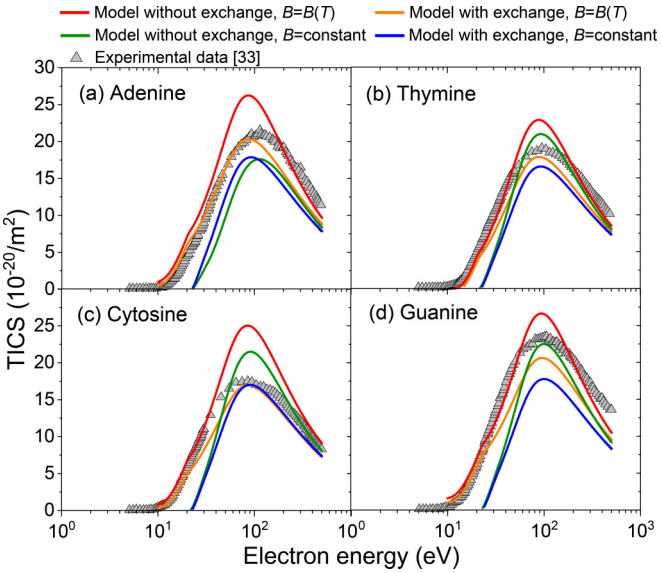

FIG. 2. Comparison of the theoretical TICSs under different assumptions in the extended model with experimental data of the four DNA bases of (a) adenine, (b) thymine, (c) cytosine, and (d) guanine. The gray triangles are the experimental measurement data adapted from Ref. [33].

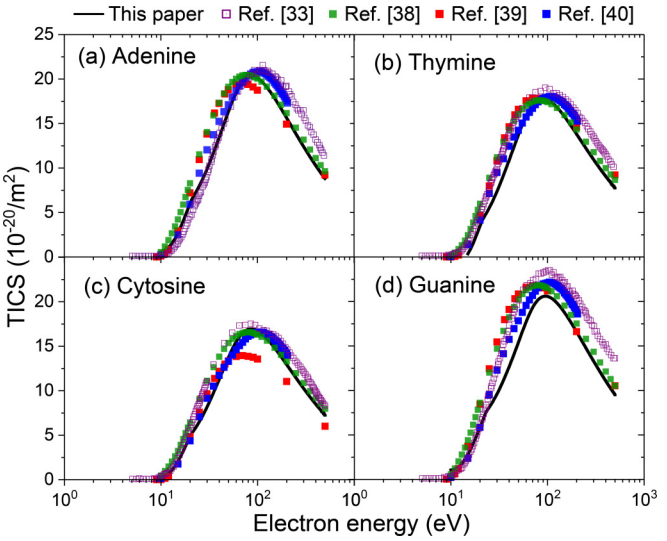

FIG. 3. Comparison of the TICSs calculated using the new semiempirical method with other theoretical calculations and experimental data for (a) adenine, (b) thymine, (c) cytosine, and (d) guanine. The solid line represents the calculation derived in this paper. The theoretical data of green, red, and blue squares are adapted from Refs. [38], [39], and [40], respectively. The empty squares are experimental measurement data adapted from Ref. [33].

[38–40] [Refs. [38,40] use the binary encounter Bethe method (BEB) but with different electronic structure input while Ref. [39] uses the complex scattering potential-ionization contribution method (CSP-ic) method]. The results are shown in Fig. 3. Despite the simplicity of this new method which involves just a few input parameters of the organic molecules, we have been able to derive the TICS curves for the DNA bases that are of similar accuracy with other theoretical methods. As we can see in Fig. 3, the magnitude and peak position of the TICS derived from our method are comparable with those from the experiment and other theoretical methods. The calculated TICSs agree with the experimental data [33] throughout the entire energy range with guanine having the highest deviation of only about 10% in the higher energy region.

This method was also applied to the calculation of the TICS of less biologically relevant organic molecules to provide greater evidence for its accuracy. The result is then compared with theoretical and experimental measurements where available. The experimental results were all measured in the gaseous phase. Figure 4 shows the TICS of aromatic organic molecules—benzene, phenol, and toluene—with data taken from different sources. The relative magnitudes of the TICS of these three compounds agree with theoretical calculation of Ref. [41] (using multiscattering center spherical complex optical potential method) with toluene having the highest TICS, followed by phenol and then benzene. For these compounds, our calculation yields a higher TICS compared to that of Ref. [41] (the highest being 20% above for benzene), whereas our calculation for benzene agrees well with data from National Institute of Standards and Technology [42] and also with the experimental data for higher energy incidence [43]. Our calculation for toluene also agrees better with experimental data compared to that of Ref. [44]. There exists a certain ambiguity in the accepted values of the TICS of these compounds, but gen-

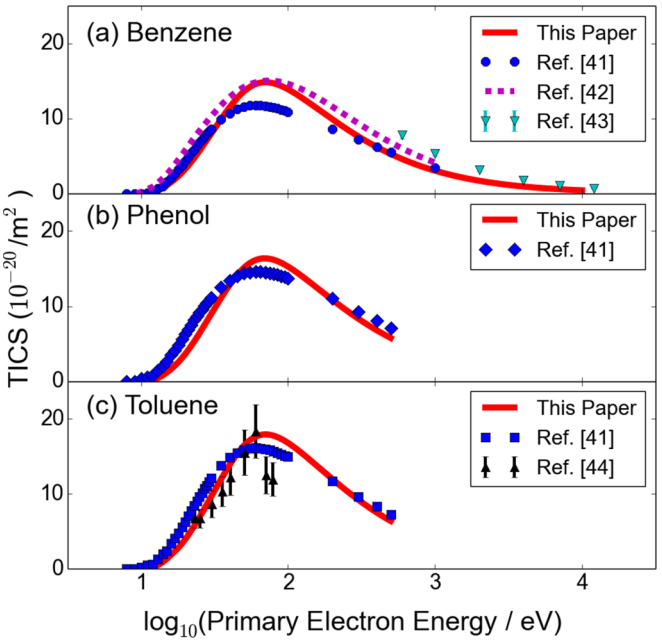

FIG. 4. Comparison of theoretical calculations of the TICSs with experimental data of three different organic compounds—benzene, phenol, and toluene. (a) The solid red line represents the TICS of benzene using our extended electron-impact model. The blue circles and dotted purple line are theoretical calculation from Refs. [41] and [42], respectively. The cyan inverted triangles are experimental data adapted from Ref. [43]. (b) The red solid line represents the TICS of phenol using our model and the blue diamonds are the theoretical calculation from Ref. [41]. (c) The red solid line is the TICS of toluene using our model and blue squares represent the theoretical calculation in Ref. [36]. The black triangles are experimental data from Ref. [44].

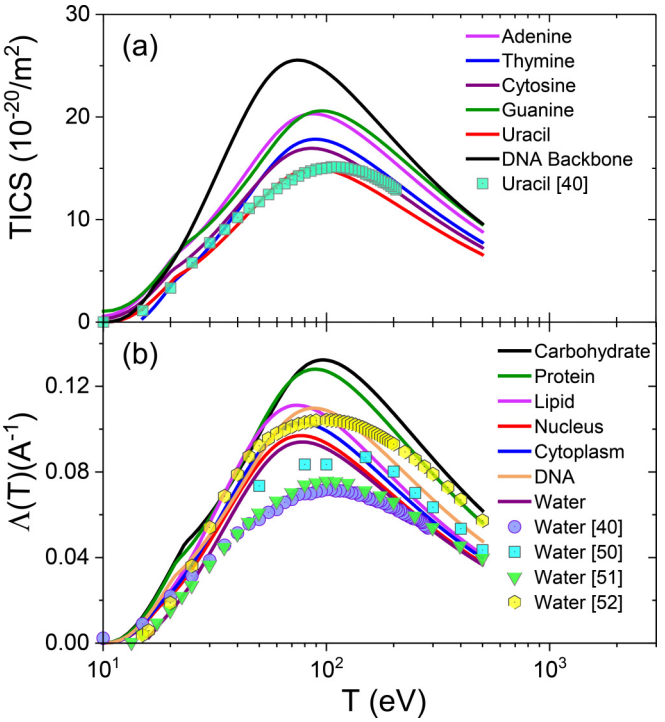

FIG. 5. (a) The solid lines show the calculated TICSs for different DNA bases (adenine, thymine, cytosine, and guanine), DNA backbones, and uracil. The solid squares are the calculated TICS data of uracil adapted from Ref. [40]. (b) The solid lines show the calculated TICSs for different biological molecules. The solid circles, squares, inverted triangles, and hexagons are the experimental measurements of the TICSs in water adapted from Refs. [40,50–52]. The experimental measurements were all made in gaseous phase, while our calculations were assumed with condensed phase of these biomolecules.

erally our results agree with theoretical and experimental data. Thus, without performing sophisticated quantum-mechanical calculation, we are able to obtain reasonably accurate estimates of the TICS of organic molecules. To summarize, this method works because most organic compounds have very similar OELF and can be parameterized using the method developed by Ref. [21], and the excitation spectrum usually dominates at the low-energy transfer region, thus reducing the errors incurred when calculating the TICS using a single mean binding energy. Due to the inherent assumptions that exists within our method, we should expect that it will not yield a TICS as accurate as much more involved theoretical models. However, given that there are more than 20,000 kinds of proteins in a cell [45], experimental measurements on all these proteins will likely not be forthcoming in the near future, and our method provides a relatively simple and reasonably accurate way to estimate their TICS for radiobiology transport simulation.

As a separate application, we used our method to find the TICS for other biological molecules (uracil, DNA, carbohydrate, etc.) to examine the sensitivity of each of these components to radiation damage. The input parameters, which include the chemical composition, atomic number, and mass number, are obtained from Ref. [25]. The binding energy for most of these molecules is approximated as $\bar{B} = (18 - 100/T)$ eV, as the information of the shell's energy of all the molecules are not available. The binding energy expression for water is deduced from Ref. [46] and is $\bar{B} = (18 - 76/T)$ eV. The results of the calculations are shown in Fig. 5. Figure 5(a) shows the comparison of the TICS of the DNA bases, uracil, and the DNA backbone. The TICS calculation of uracil from Ref. [40] is also shown in the same plot and there is excellent agreement between the method presented in this paper and that used by Ref. [40], especially in the lower-energy regime below 100 eV. In addition, the DNA backbone has the highest TICS compared to the DNA bases, which indicates that radiation damage from the direct effect will occur most readily in the backbone than in the bases. Radiation damage to the backbone can lead to DNA single-strand breaks or double-strand breaks where the latter effect accounts for reduced cell viability and increased chromosome aberrations [47–49].

Hence, from a radiobiology viewpoint, more attention should be paid to DNA strand damage compared to base damage as the backbones are the more sensitive target for secondary electrons. A comparison of the macroscopic TICS, $\Lambda(T)$ (cross section times number density), of several other compounds such as lipids, protein, carbohydrate, and water is shown in Fig. 5(b). Several experimental data [40,50–52] for water are also plotted in Fig. 5(b). The measured values of the TICS of water varied for different experiments and the calculated TICSs generally agree with experimental measurements for most of

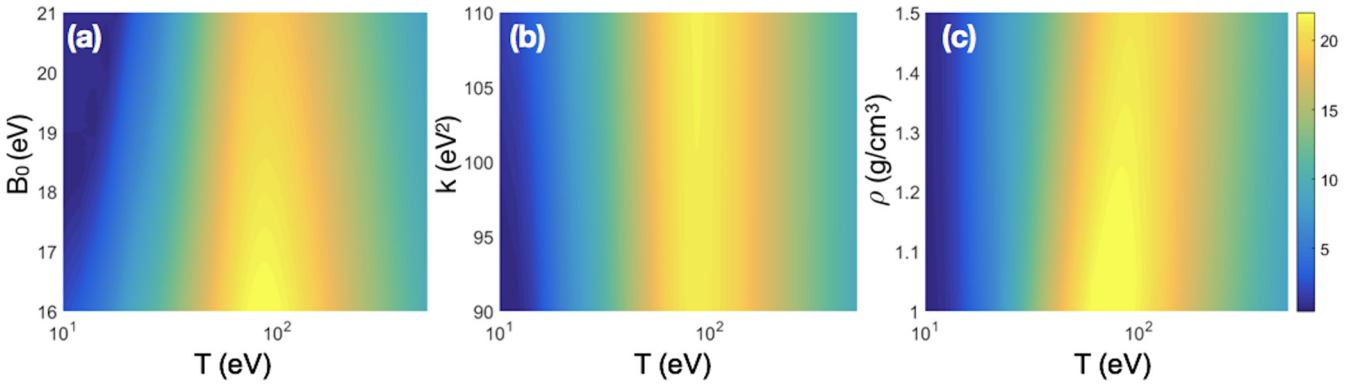

FIG. 6. Sensitivity of the TICSs with the uncertainty of the parameters (a) B_0, (b) k, and (c) ρ. The horizontal axis represents different incident electron energy and the vertical axis represents various values of the parameters, respectively while keeping other parameters constant. The color scale represents the TICS value in the unit of $\mathring{A}^2$.

the curve. However, the calculated value is higher than most experimental measurement in the low-energy regime between 20 and 100 eV. The higher TICS values from our method arise from the fact that most experimental measurements are done in the gaseous phase while TICS values in condensed phase are known to be higher than in the gaseous phase in the case of low-energy incident electrons (less than 100 eV) [53]. Also, from Fig. 5(b), most biological molecules have higher TICSs compared to water, with a difference up to 50%. Currently, most radiation transport simulation used to assess radiation damage to biological entities assume a water medium [54,55]. However, the result in Fig. 5 shows that for accurate simulation of radiation damage, one must take into account the biological composition, as this will affect the cross section, which is an important input in the simulation. In fact, from our result, any simulation done with water alone will underestimate the damage caused by secondary electrons as the TICS of most biological media is greater than that of water. It is important to note that algorithms to extract ionization and excitation cross sections from more rigorous semiempirical models of the dielectric function have been developed [56] but they significantly increase the computational burden. In particular, more rigorous methods have been used to calculate inelastic cross section (but not ionization alone as in this paper) for water and a small subset of biological materials recently [57,58], which also arrive at the same conclusion.

Even though the application of this method can be easily extended to any biomolecules, it requires certain knowledge of the molecules' chemical composition and binding energy. This information might not be readily available or might be known but only with significant uncertainty. To assess the potential of this method for practical calculation in radiotherapy or hadron therapy, one must know how such uncertainty affects the cross-section values obtained. In particular, if the model is very sensitive to a certain parameter, then it might not be useful when that parameter is only loosely known. To evaluate this, the sensitivity of TICSs on three different parameters (B_0, k, and ρ) for adenine are plotted in Fig. 6. These parameters are chosen because they are the most likely parameters to have uncertainty in their values in practice. Each of the figures in Fig. 6 is obtained by calculating the TICS at various incident electron energy for different values of the parameter, P, ranging from $0.9P$ to $1.1P$ (about 10% variation) where $P = B_0,\ k,\ \rho$. For instance, in Fig. 6(a), the TICSs for electrons are calculated for a range of B_0 values from 16 to 21 eV and for various incident energy from 10 to 500 eV. The magnitude of TICS is represented by the color scale and the figure shows how the parameters affect the TICS curves. In particular, Fig. 3(a) shows a slice of Fig. 6(a) at $B_0 = 18$ eV.

The binding energy expression in our semiempirical formalism requires two input parameters k and B_0. As shown in Fig. 6(b), the TICS values (presented with different colors) are relatively insensitive to the values of k for a 10% uncertainty in the k value. However, a 10% uncertainty in B_0 significantly affects the low-energy portion of the TICS as can be seen in Fig. 6(a). Last, Fig. 6(c) shows that uncertainty in the ρ parameters affects mainly the peak energy position of the TICS. Hence, from this analysis, B_0 and ρ values have a relatively larger impact on the TICS values and should be known with relative accuracy for any practical evaluation of the cross section of electron impact ionization on biomolecules.

V. CONCLUSION

The semiempirical method first proposed in Refs. [8,25] is a powerful technique to estimate the proton-impact ionization cross section for biomolecules with minimal input information, making the method useful for modeling and simulation in radiation therapy for cancer. In this paper, we extended the method to electron-impact ionization. By adding exchange interaction and binding energy correction to the original method, we showed that the TICSs obtained for DNA bases and other aromatic compounds agree well with both experimental and other theoretical data. In addition, we performed an assessment of our method's sensitivity to uncertainty in input parameters. In conclusion, this method provides a reasonable estimation of the TICS of organic molecules of any composition and could potentially provide the best estimates for cross-sectional values used in radiation transport simulation in biological medium where experimental measurements are absent or meager.

ACKNOWLEDGMENT

This research was funded by a National Research Foundation Singapore—Competitive Research Programme (NRF-CRP17-2017-05).

[1] W. D. Newhauser and R. Zhang, Phys. Med. Biol. **60**, R155 (2015).
[2] H. Nikjoo, D. Emfietzoglou, T. Liamsuwan, R. Taleei, D. Liljequist, and S. Uehara, Rep. Prog. Phys. **79**, 116601 (2016).
[3] E. L. Alpen, *Radiation Biophysics* (Academic Press, San Diego, CA, 1997).
[4] Z. Cai, P. Cloutier, D. Hunting, and L. Sanche, Radiat. Res. **165**, 365 (2006).
[5] M. Dingfelder, Health Phys. **103**, 590 (2012).
[6] D. Alloni, Scientifica Acta **1**, 164 (2007).
[7] H. Nikjoo, S. Uehara, D. Emfietzoglou, and F. A. Cucinotta, Radiat. Meas. **41**, 1052 (2006).
[8] P. de Vera, R. Garcia-Molina, I. Abril, and A. V. Solov'yov, Phys. Rev. Lett. **110**, 148104 (2013).
[9] P. de Vera, R. Garcia-Molina, and I. Abril, Phys. Rev. Lett. **114**, 018101 (2015).
[10] Z. Kuncic, Biophys. Rev. Lett. **10**, 25 (2015).
[11] B. Boudaiffa, P. Cloutier, D. Hunting, M. A. Huels, and L. Sanche, Science **287**, 1658 (2000).
[12] E. Alizadeh, A. G.Sanz, G. Garcia, and L. Sanche, J. Phys. Chem. Lett. **4**, 820 (2013).
[13] N. Bohr and J. Lindhard, K. Dan. Vidensk. Selsk. Mat. Fys. Medd. **28** (1954).
[14] M. Dingfelder, D. Hantke, M. Inokuti, and H. G. Paretzke, Radiat. Phys. Chem. **53**, 1 (1998).
[15] M. Dingfelder, M. Inokuti, and H. G. Paretzke, Radiat. Phys. Chem. **59**, 255 (2000).
[16] H. T. Nguyen-Truong, Appl. Phys. Lett. **108**, 172901 (2016).
[17] H. T. Nguyen-Truong, J. Phys.: Condens. Matter **29**, 215501 (2017).
[18] H. Nikjoo, W. Uehara, and D. Emfietzoglou, *Interaction of Radiation with Matter* (CRC Press, Boca Raton, FL, 2012).
[19] H. Hayashi, N. Watanabe, Y. Udagawa, and C. Kao, Proc. Natl. Acad. Sci. USA **97**, 6264 (2000).
[20] L. C. Emerson, M. W. Williams, I. Tang, R. N. Hamm, and E. T. Arakawa, Radiat. Res. **63**, 235 (1975).
[21] Z. Tan, Y. Xia, X. Liu, M. Zhao, Y. Ji, F. Li, and B. Huang, Radiat. Environ. Biophys. **43**, 173 (2004).
[22] Z. Tan, Y. Xia, M. Zhao, X. Liu, F. Li, and B. Huang, Nucl. Instr. and Met. B **222**, 27 (2004).
[23] M. Altarelli and D. Y. Smith, Phys. Rev. B **9**, 1290 (1974).
[24] B. L. Henke *et al.*, At. Data Nucl. Data Tables **54**, 181 (1993).
[25] P. de Vera, I. Abril, R. Garcia-Molina, and A. V. Solov'yov, J. Phys.: Conf. Ser. **438**, 012015 (2013).
[26] G. G. Gomez-Tejedor and M. C. Fuss, *Radiation Damage in Biomolecular Systems* (Springer, Berlin, 2012).
[27] D. Emfietzoglou, I. Kyriakou, I. Abril, R. Garcia-Molina, and H. Nikjoo, Int. J. Radiat. Biol. **88**, 22 (2012).
[28] I. Abril, R. Garcia-Molina, C. D. Denton, I. Kyriakou, and D. Emfietzoglou, Radiat. Res. **175**, 247 (2011).
[29] I. Abril, C. D. Denton, P. de Vera, I. Kyriakou, D. Emfietzoglou, and R. Garcia-Molina, Nucl. Instrum. Methods B **268**, 1763 (2010).
[30] D. Emfietzoglou, I. Kyriakou, R. Garcia-Molina, and I. Abril, Surf. Interface Anal. **49**, 4 (2017).
[31] D. Emfietzoglou, I. Kyriakou, R. Garcia-Molina, and I. Abril, J. Appl. Phys. **114**, 144907 (2013).
[32] D. Emfietzoglou, I. Kyriakou, R. Garcia-Molina, I. Abril, and H. Nikjoo, Radiat. Res. **180**, 499 (2013).
[33] M. A. Rahman and E. Krishnakumar, J. Chem. Phys. **144**, 161102 (2016).
[34] R. H. Ritchie, R. N. Hamm *et al.*, *Physical and Chemical Mechanisms in Molecular Radiation Biology* (Plenum Press, New York, 1991), p. 99.
[35] P. Berhardt and H. G. Paretzke, Int. J. Mass Spectrom. **223-224**, 599 (2003).
[36] Y. K. Kim and M. E. Rudd, Phys. Rev. A **50**, 3954 (1994).
[37] M. Michaud, M. Bazin, and L. Sanche, Int. J. Radiat. Biol. **88**, 15 (2012).
[38] P. Mozejko and L. Sanche, Radiat Environ. Biophys **42**, 201 (2003).
[39] M. Vinodkumar, C. Limbachiya, M. Barot, M. Swadia, and A. Barot, Int. J Mass Spectrom. **339-340**, 16 (2013).
[40] J. Bull, J. W. Lee, and C. Vallance, Phys. Chem. Chem. Phys. **16**, 16 (2014).
[41] S. Singh, R. Naghma, J. Kaur, and B. Antony, J. Chem. Phys. **145**, 034309 (2016).
[42] Y. K. Kim and K. K. Irikura, AIP Conf. Proc. **543**, 220 (2000).
[43] B. L. Shram, M. J. V. der Wiel, F. J. de Heer, and H. R. Moustafa, J. Chem. Phys. **44**, 49 (1966).
[44] J. R. Vacher, F. Jorand, N. Blin-Simiand, and S. Pasquiers, Chem. Phys. Lett. **434**, 188 (2007).
[45] M. S. Kim *et al.*, Nature **509**, 575 (2014).
[46] C. Champion, J. Hanssen, and P. A. Hervieux, J. Chem. Phys. **117**, 197 (2002).
[47] M. E. Lomax, L. K. Folkes, and P. O'Neill, Clin. Oncol. **25**, 578 (2013).
[48] B. D. Loucas, M. Durante, S. M. Bailey, and M. N. Cornforth, Radiat. Res. **179**, 9 (2013).
[49] D. Pang, J. E. Rodgers, B. L. Berman, S. Chasovskikh, and A. Dritschilo, Radiat. Res. **164**, 755 (2005).
[50] H. C. Straub, B. G. Lindsay, K. A. Smith, and R. F. Stebbings, J. Chem. Phys. **108**, 109 (1998).
[51] M. A. Bolorizadeh and M. E. Rudd, Phys. Rev. A **33**, 882 (1986).
[52] M. V. V. S. Rao, I. Iga, and S. K. Srivastava, J. Geophys. Res. **100**, 26421 (1995).
[53] C. Champion, Phys. Med. Biol. **55**, 11 (2010).
[54] Y. Liang, G. Yang, F. Liu, and Y. Wang, Phys. Med. Biol. **61**, 445 (2016).
[55] W. Friedland, P. Jacob, and P. Kundrat, Radiat. Prot. Dosimetry **143**, 542 (2011).
[56] I. Kyriakou, S. Incerti, and Z. Francis, Med. Phys. **42**, 3870 (2015).
[57] H. Shinotsuka, B. Da, S. Tanuma, H. Yoshikawa, C. J. Powell, and D. R. Penn, Surf. Interface Anal. **49**, 238 (2017).
[58] R. Garcia-Molina, I. Abril, I. Kyriakou, and D. Emfietzoglou, Surf. Interface Anal. **49**, 11 (2017).